Journal of the Oceanographical Society of Japan
Vol. 40, pp. 46 to 56, 1984

Internal Flow Structure of Short Wind Waves
Part 4. The Generation of Flow in Excess of the Phase Speed*

Kuniaki Okuda†

Abstract: The minimum value of wind stress under which the flow velocity in short wind waves exceeds the phase speed is estimated by calculating the laminar boundary layer flow induced by the surface tangential stress with a dominant peak at the wave crest as observed in previous experiments. The minimum value of the wind stress is found to depend strongly on β, the ratio of the flow velocity just below the boundary layer and the phase speed, but weakly on L, the wavelength. For wind waves previously studied ($\beta=0.5$, $L=10$ cm), the excess flow appears when the air friction velocity u_* is larger than about 30 cm sec^{-1}. The present results confirm that the excess flow found in my previous experiments is associated with the local growth of a laminar boundary layer flow near the wave crest.

1. Introduction

In Part I of this study (Okuda, 1982a) characteristic features of short wind waves were described on the basis of detailed measurements of the internal velocity field relative to individual wave crests. An interesting feature is that dominant waves with wave heights comparable with or larger than the mean generally accompany the flow in excess of the phase speed, though the wind speed is rather low (the air friction velocity u_* is 30 cm sec^{-1}) so that severe wave breaking accompanied by bubble entrainment never occurs. This indicates that, in short wind waves, wave breaking prevails even under conditions of low wind speed where air bubble entrainment does not occur. The purpose of this paper is to provide an appropriate interpretation for the generation of wave breaking in wind waves studied previously by the present author (Part I).

The prevalence of wave breaking in short wind waves was first predicted theoretically by Banner and Phillips (1974) by studying the effect of the drift current which inevitably coexists with wind waves. They considered that, when wind blows across the water surface, a viscous flow with great velocity shear and a thickness of several millimeters, called "surface drift", is established along the water surface, and they examined the evolution of this viscous flow along the wave surface by neglecting the effect of the viscous force which is exerted by surface tangential stress variations. Their estimations by use of the measurements made by Wu (1975) suggest that surface drift is intensified greatly at the crest by the effect of wave motions, and wave breaking, which begins when the flow velocity equals the phase speed, occurs at much smaller steepness than Stokes limit, even under the conditions of a moderate wind speed. In their model, since the surface tangential stress is assumed as being constant along the water surface, the vorticity of the surface drift remains constant along the water surface, and the augmentation of the flow velocity at the crest occurs only through thicknenning of the surface drift.

The measurements described in Part I, however, show that the characteristics of flow below such wind waves differ substantially from those assumed in Banner and Phillips' model, and suggest that the occurrence of the excess flow is associated with a different mechanism from that proposed by Banner and Phillips. As shown in Part I and also in Okuda *et al.* (1977), the surface tangential stress varies greatly along the wave profile. The stress values near the crest attain several times the wind stress determined from the mean wind profile, while the values are more or less zero on other parts of the wave. The thickness of the viscous layer is generally much smaller than that assumed by Banner and Phillips, and the thickness as well

* Received 12 July 1982; in revised form 22 September 1983; accepted 31 October 1983.

† Geophysical Institute, Faculty of Science, Tohoku University, Sendai 980, Japan.

as the vorticity in the viscous layer vary greatly along the water surface, and are closely associated with variations in the surface tangential stress. Near the crest where intense tangential stress is imposed, the vorticity in the viscous layer is extremely large, and, although the thickness of the viscous layer near the crest is only 0.2~0.3 mm, the surface velocity is greatly augmented in this region. Wave breaking in short wind waves seems to be associated with this intense viscous flow near the crest generated locally by the intense tangential stress; this viscous flow is hereafter referred to as "skin flow", in order to distinguish it from the surface drift studied by Banner and Phillips.

To show the importance of skin flow more clearly, the previous measurements of the surface tangential stress τ and the surface velocity U_s distributions for Case IV of Part I are presented in Fig. 1. For Case IV the wave steepness is small (0.045), and excess flow is not formed, unlike the case of dominant waves. The abscissa is the phase defined as 0° at the crest, −180° at the windward trough and 180° at the leeward trough. Both τ and U_s have dominant peaks near the crest. The peak value of τ, though it is considerably smaller than that for dominant waves, attains about three times the wind stress determined from the mean wind profile $\rho_a u_*^2$, where ρ_a is the air density and u_* the air friction velocity. The value of U_s increases abruptly just leeward of the crest, attains a maximum value a little windward of the crest (−30°) and suddenly decreases at a point on the windward side (−50°), and is closely syncronized with variations in the surface tangential stress. As described in Part I, this feature of U_s is associated with the evolution of skin flow near the crest. The thickness of skin flow is less than 0.5 mm, but at −30°, where the peak value of U_s occurs, the skin flow augments the surface velocity by 9–10 cm sec^{-1}, which is comparable with the intensity of underlying turbulent vortical flow with a thickness of about 3 mm and a velocity of 8–9 cm sec^{-1}, and is larger than the amplitude of orbital motion at the mean water surface level, 4.5 cm sec^{-1}. This indicates that the skin flow plays a very significant role in augmentation of the surface velocity near the crest.

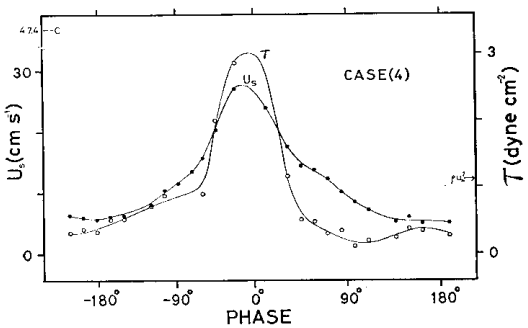

Fig. 1. Distributions of the surface tangential stress τ and the surface velocity U_s for Case IV previously studied in Part I (Fig. 7c in Okuda, 1982a). $\rho_a u_*^2$ denotes the wind stress determined from the mean wind profile and C the phase speed.

In subsequent sections I examine the growth of skin flow near the crest, and assess the effect of skin flow growth on the generation of wave breaking in short wind waves. The flow induced by the varying surface tangential stress has also been studied by Longuet-Higgins (1969) for the case of small tangential stress variations, and Uji (1979) within a linear framework, in order to examine the effect of varying tangential stress on wind wave growth. In this study I calculate numerically the skin flow induced by a similar tangential stress to that shown in Fig. 1 incorporating non-linear effects, and estimate the minimum wind stress which can generate a flow velocity equal to the phase speed. The present results confirm that the excess flow over phase speed found in the previous measurements is associated with the local growth of skin flow near the crest.

2. Formulation of the problem

2.1. Preliminary considerations

The problem of concern is the effect of skin flow on the generation of wave breaking in short wind waves. To discuss this problem, let us consider an unbroken uniform wave train exposed to a surface tangential stress distribution similar to that described in previous measurements (Part I). In this section, in order to construct an appropriate model for describing the skin flow growth, some features of skin flow under these conditions are qualitatively discussed.

The situation to be studied is schematically represented in Fig. 2. The surface tangential stress τ' varies only in the wind direction, and

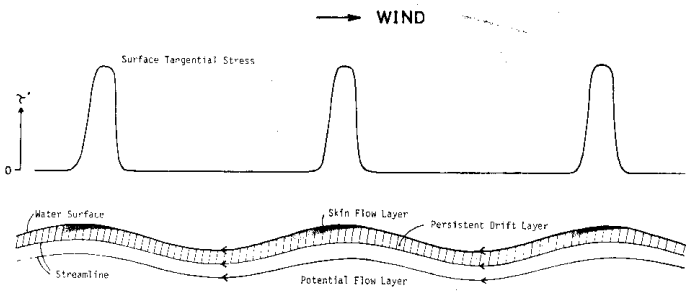

Fig. 2. A schematic representation of flow in unbroken waves which are exposed to surface tangential stress with peaks in stress near individual crests.

¡t is large in a narrow region near the wave crest and effectively zero in other regions. It is assumed that both wave profiles and the surface tangential stress distributions propagate in space approximately preserving their patterns so that they are in a quasi-steady state in a frame of reference moving with phase speed C. In this frame, since we are now concerned with unbroken waves, water elements near the water surface move along the water surface from right to left.

Under the τ' distribution being studied, water elements near the water surface acquire vorticity and momentum intermittently when they are below regions of large τ' near crests. The acquisition of vorticity and momentum begins a little leeward of the crest where τ' abruptly increases, and continues until the water elements pass the region of large τ'. By this process the skin flow which supports large velocity shear is developed below the region of large τ'. However, under these conditions of fetch limited growth, the skin flow is predicted to remain thin and laminar.

The skin flow will become obscured a little windward of the crest, where τ' decreases abruptly. After passing the large stress region, the water elements at and just below the water surface will soon loose their vorticity due to retardation by viscous forces. At the same time, the vertical diffusion of vorticity results in a deepening of the skin flow and a weakening of the vorticity in the skin flow layer. The turbulence which is generated associated with the thickening of the skin flow may also play an important role in the dissipation of the skin flow. It is thus predicted that, through these processes, the skin flow which is developed near the crest will have lost its identity almost completely somewhere near the trough.

The above mentioned growth and dissipation stages occur in individual waves so that skin flows with similar structures are predicted to be formed in individual waves as in Fig. 2. Below the skin flow layer a rather persistent turbulent drift may be supported by the momentum transfer associated with the above mentioned evolutional process of skin flow. However, the vorticity in this layer is predicted to be much weaker than that in the skin flow layer near the crest, and the time and spatial scales of evolution of this turbulent drift are much larger than the wave period and wavelength, respectively. For breaking waves with excess flow over phase speed, this drift layer also shows a distinct phase-locked structure as shown in Part I.

In the present study we are interested, not in the entire process of skin flow evolution, but only in growth of the skin flow near the crest. The above mentioned features suggest that, for the growth stage, we can construct a simple model appropriate to the present purpose. The quasi-periodic feature of skin flow together with the large time and spatial scales of evolution of the underlying drift layer suggest the possibility of studying the growth stage independently without investigating the long process of evolution of the flow near the water surface. In the growth stage the skin flow is predicted to remain thin and laminar, which suggests that the growth stage of skin flow can be described by using the equations for a laminar boundary layer without any assumptions about the characteristics of turbulence near the water surface.

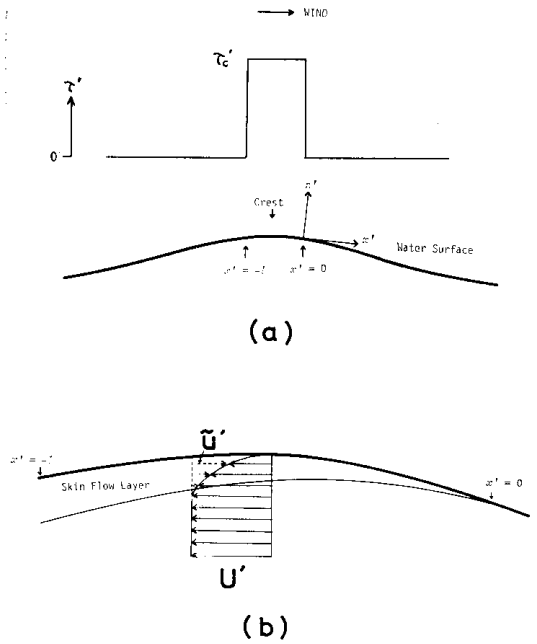

Fig. 3. (a) The assumed surface tangential stress distribution. (b) The flow near the water surface observed in a frame of reference moving with the wave profile.

2.2. Equations governing skin flow growth

We now focus our attention on a narrow region near the crest and study skin flow growth under a constant surface pressure and with surface tangential stress in the form shown in Fig. 3a. The surface tangential stress τ' is τ_c' in the region $-l \leqq x' \leqq 0$ and zero in the other regions, where x' is the distance measured leeward along the water surface, and z' the distance upward normal to the water surface. On the basis of previous measurements (Fig. 7 in Part I), the width of the large tangential stress region l is assumed to be

$$\frac{l}{L} = 0.134,$$

where L is the wavelength. The skin flow actually grows under a free surface so that the configuration of the water surface in the absence of skin flow is altered by the growth of skin flow. The growth of skin flow may be affected by the pressure field associated with this variation of water surface configuration induced by the growth of the skin flow itself. However, this effect is not incorporated in the present study; as will be discussed in Section 5, the neglection of this effect is justifiable for conservative estimate of the effect of skin flow. Thus, the water surface, which is specified by $z'=0$, is assumed a priori to have the form of a sinusoid with a crest at $x' = -\frac{l}{2}$.

Figure 3b shows a schematic representation of the flow near the crest. $\tilde{u}'$ and U' are the x' components of the skin flow and the flow just below the skin flow layer, respectively. It is supposed that motion occurs in the (x', z') plane and is quasi-steady in the frame used here. The skin flow is assumed to remain laminar in the region being considered. The underlying flow U' is a resultant of wave motion, the underlying rather persistent drift (Fig. 2) and the movement of the frame. The underlying drift is generally vortical and the intensity varies in both x'- and z'-directions. However, the spatial scale of evolution of this flow is much larger than l, and the vorticity is much weaker than that in the skin flow layer; the vorticity just below the skin flow layer is predicted to be equivalent to that near the water surface leeward of the crest, which is zero in the present situation. Therefore, the underlying drift can be assumed to be uniform in the region considered. For wave motion, since the thickness of the skin flow layer is much smaller than L, the variation in the z'-direction is neglected. In the present study, the underlying flow U' thus varies only in the x'-direction associated with wave motion, and is specified a priori. We denote the average magnitude of $|U'|$ over $-l \leqq x' \leqq 0$ as U_0'.

Since the skin flow is assumed to be laminar, the full equation of motion are the Navier-Stokes equations and the continuity equation. However, according to the boundary layer theory, the full equations reduce to so-called the boundary layer equations, when the thickness of flow δ is sufficiently small, that is

$$\frac{\delta}{l_s} \ll 1,$$

where l_s is a length scale characterizing the variation of flow in the x'-direction, and is l in the present case. For the skin flow being considered, $\delta \sim \left(\frac{\nu l}{U_0'}\right)^{1/2}$, where ν is the viscosity of water, as predicted from the solution of the linearized equations of motion for a laminar boundary layer flow induced under a constant

surface tangential stress. Thus,

$$\frac{\delta}{l}\sim R^{-1/2},$$

where $R=\frac{l\bar{U}_0'}{\nu}$ is the Reynolds number. In the present study we consider the situation $10^3<R<10^5$, so that we can use the boundary layer equations as basic equations for the skin flow.

We denote x' and z' components of flow velocity in the skin flow layer as u' and w', respectively. The pressure is denoted as p', and we introduce $P=\frac{p'}{\rho}+gh'$, where h' is the distance measured vertically upward from the mean water surface level of the wave field to the water surface, ρ the density of water and g the acceleration due to gravity. As usual, we introduce non-dimensional variables:

$$x=x'/l, \quad z=R^{1/2}z'/l, \quad u=u'/\bar{U}_0', \quad w=R^{1/2}w'/\bar{U}_0', \quad U=U'/\bar{U}_0', \quad P=P'/\bar{U}_0'^2.$$

Boundary layer equations for flow over a curved surface as in the present situation have been derived by Jones and Watson (1963), and were shown to have the same form as for flow over a flat surface, when $R\gg 1$. In non-dimensionalized forms, they are

$$u\frac{\partial u}{\partial x}+w\frac{\partial u}{\partial z}=-\frac{\partial P}{\partial x}+\frac{\partial^2 u}{\partial z^2}, \qquad (1)$$

$$\frac{\partial u}{\partial x}+\frac{\partial w}{\partial z}=0. \qquad (2)$$

The equation of motion in the z-direction is

$$\frac{\partial P}{\partial z}=\kappa l R^{-1/2}u^2,$$

where κ is the curvature of the water surface. However, in the situation being considered, $\kappa l\ll 1$ so that the above equation reduces to

$$\frac{\partial P}{\partial z}=0.$$

This equation implies that across the skin flow layer there is no variation in P so that P is determined by the conditions of flow just below the skin flow layer. From Bernoulli's theorem for a streamline just below the skin flow layer, which is, to the approximation used here, parallel with the water surface, we obtain

$$\frac{\partial P}{\partial x}=-U\frac{dU}{dx}.$$

Thus, Eq. (1) can be rewritten as

$$u\frac{\partial u}{\partial x}+w\frac{\partial u}{\partial z}=U\frac{dU}{dx}+\frac{\partial^2 u}{\partial z^2}. \qquad (3)$$

The flow must satisfy the following boundary conditions. The water surface is assumed as being fixed, and the surface tangential stress must have a prescribed value so that the velocity must satisfy

$$w=0 \text{ at } z'=0, \qquad (4a)$$

$$\left(\frac{\partial u}{\partial z}\right)_s=\frac{R^{1/2}\tau_c'}{\rho\bar{U}_0'^2}, \qquad (4b)$$

where $(\ )_s$ shows the value at $z=0$. The flow velocity in the skin flow layer must join smoothly with that outside it. Thus

$$u(x,z)\to U(x) \text{ as } z\to-\infty. \qquad (5)$$

Finally, the velocity profile must be specified at an initial section, say at $x=0$. At $x=0$ the skin flow has not yet been developed so that the velocity profile at $x=0$, $u(0,z)$, is

$$u(0,z)=U(0). \qquad (6)$$

As discussed previously, the underlying flow $U'(x')$ is the resultant of wave motion, the uniform drift and the movement of the frame. By assuming small steepness for the wave being considered, the flow can be represented as

$$U'(x')=a\sigma\cos\frac{2\pi}{L}\left(x'+\frac{l}{2}\right)+U_D'-C, \qquad (7)$$

where a is the amplitude, σ the frequency and U_D' is the drift velocity (constant). In Eq. (7) $a\sigma\cos\frac{2\pi}{L}\left(x'+\frac{l}{2}\right)+U_D'$ is the velocity measured in a spatially fixed frame. Its average value over $-l\leqq x'\leqq 0$ is denoted as $\bar{U}_c'(=C-\bar{U}_0')$, and $\bar{U}_c'/C$ as β. Since $l/L=0.134$, the non-dimensional form of Eq. (7) is written, by use of β, as

$$U=\frac{1.03\beta(1-\gamma)}{1-\beta}\cos\{0.8419(x+0.5)\}+\frac{\beta\gamma}{1-\beta}-\frac{1}{1-\beta}, \qquad (8)$$

where $\gamma=\frac{U_D'}{\bar{U}_c'}$ is the ratio of drift velocity to $\bar{U}_c'$.

In the present calculation, our main concern is to estimate τ_{crit}, the minimum value of the non-dimensionalized surface tangential stress which can develop a skin flow with $u_s=0$ somewhere in the region $-1\leqq x\leqq 0$, where $u_s(\equiv u(x,0))$ is the surface velocity. As seen from the functional form of U, the value of τ_{crit} is generally dependent both on β, the averaged magnitude of the underlying flow velocity divided by the phase speed, and γ, which designates the characteristics of the underlying flow. In the present study we estimate τ_{crit} for two cases of γ, regarding β as a parameter in each of them, as follows:

(A) $\gamma=1$

This is the case where the wave slope is extremely small, and the underlying flow in a spatially fixed frame consists solely of the uniform drift. In this case

$$U=-1, \qquad (9)$$

from Eq. (8), and there is no pressure variation. In this case, since U is constant, τ_{crit} has a constant value regardless of the value of β, as will be described in Section *3.2*.

(B) $\gamma=0.3$

For the conditions previously studied (Part I), the amplitude of orbital velocity at the water surface is equivalent to the drift velocity, that is, $\gamma\sim 0.5$, but in this case a considerably larger orbital velocity is assumed. In this case the orbital velocity constitutes on average 70 % of $\bar{U}_c'$. From Eq. (8)

$$U=\frac{\beta}{1-\beta}[0.7211\cos\{0.8419(x+0.5)\}+0.3]-\frac{1}{1-\beta}. \qquad (10)$$

In this case U is a function of β so that τ_{crit} is dependent on β. We estimate τ_{crit} for $\beta=0.3$, 0.5 and 0.7.

In later sections, it will be shown that, for the same value of β, τ_{crit} differs only a little between Cases A and B, which indicates that the effects of variation of the underlying flow and pressure variation are secondary for skin flow growth. Therefore, by studying the above two extreme cases of γ, we can safely estimate approximate values of τ_{crit} without precise knowledge of γ.

3. Calculation methods

3.1. Step-by-step method

The method of numerical solution of a laminar boundary layer flow has been developed by many workers (Gadd *et al.*, 1963). Among the existing methods, the numerical step-by-step method developed by Leigh (1955) is used for the present calculation.

We suppose that the solution u at x_1 is known and is denoted by u_1, and we wish to find the solution u_2 at the neighbouring point $x_2=x_1-\Delta x$, where Δx is positive. From Eqs. (2) and (3), by replacing derivatives in the x-direction by finite differences and putting $q=u_1+u_2$, we obtain

$$q_{zz}-\frac{1}{\Delta x}\left\{\int_0^z(q-2u_1)dz\right\}q_z+\frac{1}{\Delta x}q(q-2u_1)=-\left\{\left(U\frac{dU}{dx}\right)_{x=x_1}+\left(U\frac{dU}{dx}\right)_{x=x_2}\right\}, \qquad (11)$$

where the suffix z denotes the differentiation in the z-direction. The boundary conditions for q are

$$q_z=\frac{2R^{1/2}\tau_c'}{\rho\bar{U}_0'^2} \quad \text{at} \quad z=0, \qquad (12)$$

$$q=U(x_1)+U(x_2) \quad \text{at} \quad z=-\infty. \qquad (13)$$

The above equation and the conditions, except for Eq. (12), are the same as those used by Leigh, and, by replacing derivatives in the z-direction by suitable difference quotients, the solution q can be obtained by the iterative method described by Leigh. Thus, if the initial profile is specified at a point $x=x_1$, we can know the subsequent development of skin flow by advancing the above calculation from $x=x_1$ toward $x=-1$.

For detecting the initial growth process of skin flow completely, the profile must be specified at $x=0$ as in Eq. (6), and the calculation must be advanced from $x=0$. However, the thickness of the skin flow is zero at $x=0$ so that the above method cannot be applied to the region very close to $x=0$. To overcome this computational difficulty, the above calculation was advanced from $x=-\Delta$, where Δ is positive and $\Delta\ll 1$, by specifying an appropriate profile at $x=-\Delta$. The velocity profile at $x=-\Delta$ was

specified in the form predicted from the analytical solution of the linearized equation of motion for Case A

$$-\frac{\partial u}{\partial x}=\frac{\partial^2 u}{\partial z^2},$$

since, near $x=0$, the skin flow velocity $\tilde{u}\simeq 0$ so that $u=\tilde{u}+U\simeq -1$. In the present calculation Δ was taken as 0.0005, and it was confirmed that further decrease of Δ has negligible effect on the solution.

The thickness of skin flow increases very rapidly with increase of $|x|$. Therefore, the z-interval of calculation points, h, was increased with the growth of skin flow, but it was kept smaller than $\delta(x)/20$, where $\delta(x)$ is the characteristic thickness of the skin flow. The total number of calculation points was 200, and the x-step interval, Δx, was taken as $\Delta x\sim h^2$, except for the region where the surface velocity $u_s\simeq 0$.

The applicability of the formulation described in Section *2.2* is limited to the situation where $u_s<0$ everywhere in the region $-1\leqq x\leqq 0$. However, to estimate τ_{crit}, the above calculation was also performed formally for $\tau=\tau_B$ under which conditions the skin flow can attain $u_s\geqq 0$. In this case the iteration diverges when u_s approaches very close to zero, and the calculation was stopped just before the occurrence of $u_s=0$. The solution was obtained in the region $x_0\leqq x\leqq -\Delta$, where x_0 is the point at which u_s increases beyond -0.001 (Case A), or -0.0005 (Case B). This formal solution does not simulate the flow which actually occurs under the prescribed tangential stress distribution, but does simulate, for example, the flow for $\tau=\tau_B$ in the region $x_0\leqq x\leqq 0$ and $\tau=0$ in the other regions, in which $u_s<0$.

The numerical solution was checked by the momentum-integral equation for an incompressible two dimensional boundary layer flow (Schlichting, 1979). The total momentum was found to be conserved within 0.01 % for Case A and 0.1 % for Case B.

3.2. Determination of τ_{crit}

The values of τ_{crit}, the minimum tangential stress which can produce $u_s=0$ somewhere in the region $-1\leqq x\leqq 0$, was determined using different methods in Cases A and B.

For Case A the underlying flow is constant and pressure variation is absent so that u increases monotonously toward $x=-1$ due to the effect of tangential stress. Therefore, τ_{crit} is the value when the solution u satisfies

$$u_s=0 \quad \text{at} \quad x=-1. \tag{14}$$

τ_{crit} may be determined by repeating the calculations and changing the value of τ, as long as the solution u satisfies the condition (14) with sufficient accuracy, but here it was determined more readily from a formal solution for $\tau\geqq\tau_{crit}$ as follows. Let us consider the situation where a stress $\tau_B\geqq\tau_{crit}$ is applied and $u_s=0$ occurs at $x=x_B(\geqq -1)$, and let us rescale the dimensional quantities by replacing l with $l_B=|x_B|l$. In Case A, the non-dimensionalized Eqs. (2) and (3), and the conditions (4a), (5) and (6) remain similar for this rescaling, and, in the situation being considered, the above conditions (14) is also satisfied. This implies that, if l_B is taken as the scaling length, u and the rescaled τ remain similar for arbitrary values of $\tau_B(\geqq\tau_{crit})$. Thus, τ_{crit} can be determined from a formal calculation for τ_B as

$$\tau_{crit}=\tau_B|x_B|^{1/2},$$

where x_B can be replaced with sufficient accuracy by x_0 mentioned in Section *3.1*.

For Case B τ_{crit} is dependent on β. In this case τ_{crit} was determined for $\beta=0.3$, 0.5 and 0.7 by repeating calculations and changing τ by small intervals $\Delta\tau$ until $u_s\simeq 0$ appears.

For Case A the accuracy of τ_{crit} is mainly governed by the computational error mentioned in Section *3.1*, which is of the order of 0.01 %. For Case B it is governed by $\Delta\tau$; the value of $\Delta\tau/(2\tau_{crit})$ in the present calculation is less than 0.002.

4. The solution for $\tau\simeq\tau_{crit}$

In this section we describe the behavior of the solutions for $\tau=\tau_{crit}$ (Case A) and for a stress marginally larger than τ_{crit} (Case B). The present solution for $\tau\geqq\tau_{crit}$ simulates the flow of unbroken waves exposed to the tangential stress decreasing to zero at a point just before the appearance of $u_s=0$, as mentioned in Section *3.2*. From these solutions for $\tau\simeq\tau_{crit}$, we can appreciate some features of skin flow growth

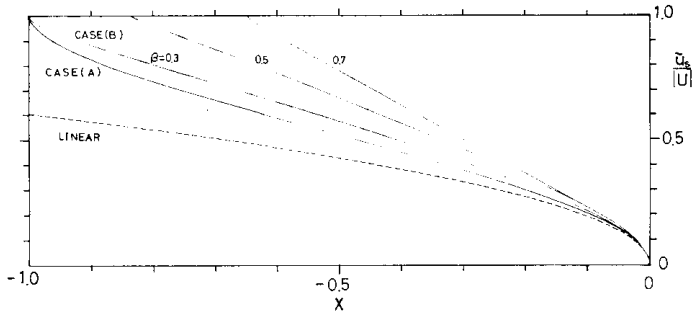

Fig. 4. The solutions for τ equal to τ_{crit} (Case A) or marginally larger than τ_{crit} (Case B). For comparison, the prediction from the linearized equation of motion under the same conditions as for Case A is shown by a dashed line.

just before the transition to the breaking state. In the present framework we cannot discuss the flow in the breaking state. However, some specific features of flow for breaking waves have been described in Part I and Part II (Okuda, 1982a, b) on the basis of experimental results.

Figure 4 shows $\tilde{u}_s(x)/|U(x)|$, where $\tilde{u}_s(x)$ $(=u(x,0)-U(x))$ is the intensity of the skin flow. For comparison, the skin flow predicted by the linearized equation under the same boundary conditions and value of τ as for Case A, is shown by a dashed line. An interesting feature is that the skin flow grows much more rapidly than the linearized equation predicts. In most of the region $\tilde{u}_s$ increases in proportion to $|x|$, and for Case A, in particular, it grows quite abruptly near $x=-1$ where zero surface velocity occurs. For Case A at $x=-1$, $\tilde{u}_s$ attains about 1.65 times the value predicted by the linearized equation of motion. Another interesting feature is the difference in the manner of growth of the skin flow between Case A and Case B. In Case A, $\tilde{u}_s/|U|=1$ occurs at $x=-1$, but for $\beta=0.5$ and 0.7 for Case B it occurs at points well before $x=-1$. In Case B the growth of skin flow near the point $\tilde{u}_s/|U|=1$ is much more gradual than in Case A.

Figure 5 shows $Q_s=U\dfrac{dU}{dx}+\left(\dfrac{\partial^2 u}{\partial z^2}\right)_s$, the value of the right hand side of Eq. (3) at the water surface, together with $\tilde{u}_s/|U|$ near the point $\tilde{u}_s/|U|=1$. For Case A, Q_s shows a large value even at the point closest to $x=-1$. The abrupt increase of $\tilde{u}_s$ near $x=-1$ is associated with this feature of Q_s, since $\dfrac{\partial \tilde{u}_s}{\partial x}=Q_s/u_s$ from

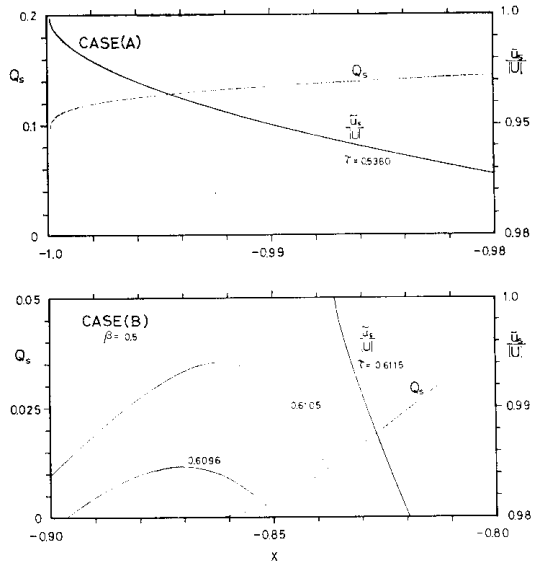

Fig. 5. The solutions near the point $u_s=0$ and $Q_s=U\dfrac{dU}{dx}+\left(\dfrac{\partial^2 u}{\partial z^2}\right)_s$ (the value of the right hand side of Eq. (3) at the water surface). In the lower panel for Case B, $\tilde{u}_s/|U|$ for $\tau=0.6105$ and 0.6096 (both smaller than τ_{crit}) is also shown. Q_s in this case is for $\tau=0.6105$.

Eq. (3). For $\beta=0.5$ for Case B, $\tilde{u}_s/|U|$ for $\tau=0.6105$ and 0.6096 (both a little smaller than τ_{crit}) is also shown by thin solid lines. For $\tau=0.6105$, $\tilde{u}_s/|U|$ shows a maximum value near $x=-0.86$, while Q_s, shown by a dashed line, decreases rapidly to zero on approaching this point as a result of canceling of $U\dfrac{dU}{dx}$ and $\left(\dfrac{\partial^2 u}{\partial z^2}\right)_s$. This may explain the gradual increase of $\tilde{u}_s$ near the point $\tilde{u}_s/|U|=1$ in Case B.

For Case A, $\tilde{u}_s$ increases very rapidly near $x=-1$ (Fig. 4). The boundary layer approximation, which is strict when $R=\infty$, is, however, also applicable in this region. For the wind waves discussed in the next section, $10^3<R<10^5$, and

$$\left(\frac{\partial^2 u}{\partial z^2}\right)_s,\ \left(u\frac{\partial u}{\partial x}\right)_s \gtrsim \frac{1}{R}\left(\frac{\partial^2 u}{\partial x^2}\right)_s$$

is satisfied up to about $x=-0.984$ (for the smallest R) and $x=-0.9995$ (for the largest R).

5. The occurrence of $u_s=0$ in short wind waves

The values of τ_{crit} estimated by the methods described in Section *3.2* and x_{crit}, the point where $u_s=0$ for $\tau=\tau_{crit}$, are listed in Table 1. The x_{crit} for $\beta=0.5$ and 0.7 of Case B is $1/2$ (x_m+x_0), where x_m is the point where $\tilde{u}_s/|U|$ reaches a maximum (Fig. 5) for $\tau=\tau_{crit}-1/2\,\Delta\tau$ and x_0 is the final calculation point for $\tau=\tau_{crit}+1/2\,\Delta\tau$ (Section *3.1*). The τ_{crit} for Case B is larger than that for Case A, which indicates that, for the same value of β, the presence of wave motion and associated pressure variation is unfavorable for skin flow growth. However, though the value of γ differs greatly between the two cases, the difference in τ_{crit} is small.

The present model, especially the surface tangential stress distribution along the wave profile, is constructed to fit the measurements for waves of $L\sim10$ cm previously studied. It is not clear whether the present model also applies to waves with much longer wavelengths, since measurements for such waves are lacking. However, to understand the applicability and the limitations of the present mechanism of wave breaking to other situations, τ'_{crit}, the dimensional value of τ_{crit} was estimated for $5\,\text{cm}\leqq L\leqq100$ cm from the values presented in Table 1. In the calculation it is assumed that the phase speed is $C=1.15\,C_0$, according to the measurements of Part III (Okuda, 1983), where C_0 is the prediction from linear theory. The local Reynolds number of skin flow $R_\delta=\bar{U}_0'\dfrac{\tilde{u}_s(x)\delta_*(x)}{\nu}$, where $\delta_*(x)$ is the displacement thickness, was at most 450, which guarantees that the skin flow remains laminar over the ranges of L and β studied in the present calculation; according to Shlichting (1979) the transition to a turbulent state occurs at $R_\delta\sim950$. As seen from Fig. 6, τ'_{crit} depends weakly on L $(\propto L^{1/4})$, but strongly on β $(\propto(1-\beta)^{3/2})$. The effectiveness of the present mechanism of wave breaking thus depends primarily on β.

Table 1. Calculated values of τ_{crit} and x_{crit} (the position of $u_s=0$).

	τ_{crit}	x_{crit}
Case A	$0.53599\pm2\times10^{-5}$	-1.0
Case B		
$\beta=0.3$	$0.5660\pm6\times10^{-4}$	-1.0
$=0.5$	$0.6110\pm5\times10^{-4}$	-0.849 ± 0.013
$=0.7$	$0.625\pm1\times10^{-3}$	-0.662 ± 0.014

For waves with $L\sim10$ cm the present mechanism is shown to be sufficiently effective to generate the excess flow. In the present model β is $\bar{U}_c'/C$, where $\bar{U}_c'$ is the sum of the orbital velocity near the crest and the drift. The value of β may vary considerably among individual waves, in particular, according to their steepness. However, for dominant waves with wave heights comparable with or larger than the mean, we can safely suppose that $\beta\gtrsim0.5$ from the measurements of Part I. From Okuda *et al.* (1977) and Part I, it is also known that for dominant waves the tangential stress near the crest can be up to more than five times the average value of wind stress $\rho_a u_*^2$. From these facts, it is predicted that for the waves previously studied ($L=10$ cm and $\beta=0.5$) $u_s=0$ occurs when $\tau_c'\gtrsim5$ dyne cm^{-2} or $\rho_a u_*^2\gtrsim1$ dyne cm^{-2}. This confirms that the generation of excess flow under the conditions of previous experiments ($u_*=30$ cm sec^{-1}) is associated mainly with

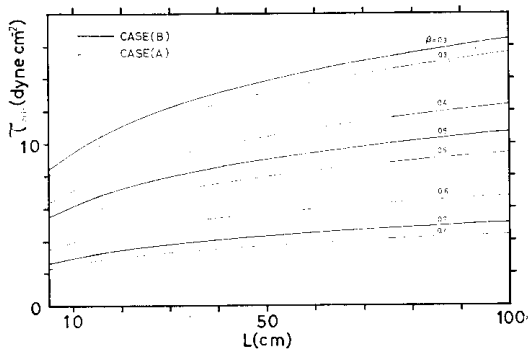

Fig. 6. Dimensional value of the minimum surface stress as a function of wavelength L for some values of β. Thin lines are for Case A and thick lines for Case B.

the local growth of skin flow near individual crests.

The above estimated value of the minimum wind stress, however, appears to be somewhat larger than that predicted from qualitative observations by use of flow visualization techniques carried out under various conditions (Okuda *et al.*, 1976); these observations suggested that the occurrence of excess flow is a general feature of short wind waves irrespective of wind speed. This may be due to the following circumstances. One is the strong dependence of τ_{crit} on β. In the actual wind wave field the value of β is predicted to vary considerably among individual waves. This implies that the minimum wind stress estimated from the average value of β does not provide a strict criterion for the appearance of waves accompanied by excess flow. Another possibility to be considered is that factors which were not incorporated in the present model take part in the growth of skin flow. In the present model the wave profile is specified a priori in the form of a sinusoid, and the effect of modification of the wave profile by skin flow growth is neglected. From Longuet-Higgins (1969), the water surface in the large stress region is predicted to be raised upward by the order of the skin flow thickness $\delta(x')$ from the level in the absence of skin flow. Therefore, the pressure force associated with this modification of the wave profile is of the order of $g\frac{\delta(-l)}{l}$, and it acts to support skin flow growth. Since $\delta(-l)/l \sim R^{-1/2}$, the effect of this pressure force is negligible when R is very large, but, under the conditions of the experiments examined here, this effect might affect the generation of the excess flow to some extent.

Acknowledgements

The author is grateful to Dr. T. Uji for his critical reading of the manuscript and comments.

References

Banner, M. L. and O. M. Phillips (1974): On the incipient breaking of small scale waves. J. Fluid Mech., **65**, 647-656.

Gadd, G.E., C.W. Jones and E.J. Watson (1963): Approximate methods of solution. In: Laminar Boundary Layer, ed. by L. Rosenhead, Oxford Univ. Press, Chap. VI.

Jones, C.W. and E.J. Watson (1963): Two-dimensional boundary layers. In: Laminar Boundary Layer, ed. by L. Rosenhead, Oxford Univ. Press, Chap. V.

Leigh, D. C. (1955): The laminar boundary-layer equation: A method of solution by means of an automatic computer. Proc. Camb. Phil. Soc. **51**, 320-332.

Longuet-Higgins, M. S. (1969): Action of variable stress at the surface of water waves. Phys. Fluids, **12**, 737-740.

Okuda, K. (1982a): Internal flow structure of short wind waves. Part I. On the internal vorticity structure. J. Oceanogr. Soc. Japan, **38**, 28-42.

Okuda, K. (1982b): Internal flow structure of short wind waves. Part II. The streamline pattern. J. Oceanogr. Soc. Japan, **38**, 313-322.

Okuda, K. (1983): Internal flow structure of short wind waves. Part III. Pressure distributions. J. Oceanogr. Soc. Japan, **38**, 331-338.

Okuda, K., S. Kawai and Y. Toba (1977): Measurements of skin friction distribution along the surface of wind waves. J. Oceanogr. Soc. Japan, **33**, 190-198.

Okuda, K., S. Kawai, M. Tokuda and Y. Toba (1976): Detailed observation of the wind-exerted surface flow by use of flow visualization methods. J. Oceanogr. Soc. Japan, **32**, 53-64.

Schlichting, H. (1979): Boundary Layer Theory. New York, McGraw-Hill.

Uji, T. (1979): Water waves induced by a fluctuating tangential stress. J. Oceanogr. Soc. Japan, **34**, 189-203.

発達初期の風波の内部構造
第4報　位相速度を越える流れの発生

奥　田　邦　明*

要旨: 波の峯でするどいピークを持つ接線応力分布のもとで発達する層流境界層流を計算し，発達初期の風波に位相速度を越える流速が発生する最小の風の応力の値を見積った．風の応力の最小値は，境界層のすぐ下の流速値と位相速度の比 β に強く依存するが，風波の波長 L には余り依存しないこと，および先に実験的に調べた風波（$\beta=0.5$, $L=10$ cm）では，位相速度を越える流速は，風の摩擦速度 u_* が約 30 cm sec^{-1} 以上のときに発生することが分かった．本報の計算結果は，先の実験で見い出された発達初期の風波における位相速度を越える流速の存在は，個々の峯付近で局所的に発達する層流境界層流に起因することを確めている．

* 東北大学理学部　地球物理学科
〒980 仙台市荒巻字青葉